New Geothermometer Based on Soil CO$_2$ Flux for Geothermal Exploration

Mark Harvey[1], Julie Rowland[1], Giovanni Chiodini[2], Clinton Rissmann[3], Simon Bloomberg[4], Thrainn Fridriksson[5], Audur Oladottir[5]

[1]School of Environment, University of Auckland, Auckland, New Zealand

[2]Istituto Nazionale di Geofisica e Vulcanologia sezione di Bologna"Osservatorio Vesuviano," Via Diocleziano, Napoli 328-80124, Italy

[3]GNS Science, New Zealand

[4]Department of Geology, Mines, and Water Resources, Private Bag PMB001, Port Vila, Vanuatu

[5]Iceland GeoSurvey, Grensasvegur 9, 108 Reykjavík, Iceland.

e-mail: mark@harveygeoscience.com

Keywords: Geothermometer, CO2, flux, exploration

ABSTRACT

We propose a new geothermometer (TCO2 Flux) based on soil diffuse CO$_2$ flux and shallow temperature measurements made on areas of steam heated, thermally altered ground above active geothermal systems. The geothermometer is based on a previous gas (CO$_2$) geothermometer. T$_{CO2}$ Flux provides an additional exploration tool for estimating subsurface temperatures in high-temperature geothermal systems. The spatial distribution of geothermometry estimates matches the location of major upflow zones previously reported at the Rotokawa (New Zealand) and Wairakei (New Zealand) geothermal systems. Mean T$_{CO2\ Flux}$ estimates fall within the range of deep drill hole temperatures at Wairakei, Rotokawa, Tauhara (New Zealand), Ohaaki (New Zealand), Reykjanes (Iceland) and Copahue (Argentina). TCO2 $_{Flux}$ was also evaluated at White Island (New Zealand) and Reporoa (New Zealand), where limited sub-surface data exists. Mode TCO2 Flux at White Island is the highest of the systems considered in this study (320 °C). However, the geothermometer relies on mineral-water equilibrium in neutral reservoir fluids, and this assumption would be violated in such an active and acidic environment. Mean TCO2 Flux at Reporoa (310 °C) is high, which suggests Reporoa is a separate system with a separate upflow from the nearby Waiotapu geothermal system.

1. INTRODUCTION

A variety of gas phase and liquid geothermometers are used in geothermal exploration and development to estimate temperatures in reservoirs (Fournier, 1977; Giggenbach, 1980; Henley et al., 1984; Arnórsson and Gunnlaugsson,1985; Giggenbach, 1988; Chiodini and Marini, 1998). Liquid geothermometers rely on the abundances of chemical species dissolved in thermal spring waters and bore waters. It follows that liquid geothermometers can only be applied where deeply sourced thermal waters flow into bore holes or can be collected from surface spring discharges. In addition, deep waters must have ascended quickly from the reservoir in order to avoid re-equilibration. Similarly, gas geothermometers rely upon the presence of accessible fumaroles; steam vents supplying a high pressure vapour discharge.

Geothermal hot springs are often of the acid-sulphate type; near surface meteoric waters that have been heated by steam. These steam-heated waters are not useful for geothermometry as they contain little of the original chemical information. Even where spring waters are deeply sourced, they may have been diluted, or have undergone geochemical re-equilibration as they flowed to the surface. Such waters may only be utilised where there are enough samples to allow development of mixing models, so that parent waters may be derived (Fournier, 1977; Arnórsson, 1985).

Similar limitations exist for gas geothermometry. Fumarole discharges will only provide reliable analysis when they are hot and vigorous (Arnórsson et al., 2006). Samples from weak fumaroles are prone to contamination. This is a consequence of the sampling methodology (evacuated flask); air may be drawn into the flask during sampling by the vacuum. Even where it is possible to avoid air contamination, fumaroles may be subject to water vapour condensation, causing an unknown enrichment of non-condensable gases in the flask. The condensation effect can be regarded as a sample size problem, which is analogous to the dilution problem in spring water geothermometry (see above); both problems might be overcome where numerous samples are available for collection, as this would allow construction of mixing/condensation models.

The scarcity of suitable springs and fumaroles contrasts with areas of steam heated ground, which are often much more common. This report presents a new method that permits an unlimited number of gas (CO2) concentration estimates on steam heated ground. The method gives large datasets that are interpreted by pre-existing CO2 geothermometers (Giggenbach, 1984; Arnórsson and Gunnlaugsson, 1985). The pre-existing geothermometers operate on the principle that the CO2 concentration in high temperature liquid reservoirs are a function of mineral-water equilibrium (temperature dependent): Plagioclase + CO2 = Clay + Calcite (Giggenbach, 1981). This report includes data from eight geothermal fields: one in Iceland (Reykjanes), one in Argentina (Copahue), and six in the Taupō Volcanic Zone (TVZ), New Zealand. The concentration of CO2 in the basalt-hosted reservoir fluids of Iceland (above 230°C) is set by the reaction: Prehnite + CO2 = Epidote + Calcite (Arnórsson et al., 1998; Stefánsson and Arnórsson, 2002). In Argentina, the Copahue volcano

produces a mixture of pyroclastics and lava flows of basaltic–andesitic composition (Agusto et al., 2013), so a similar set of reactions are expected to control the CO_2 concentration. The most common primary form of plagioclase in the TVZ is andesine (Browne and Ellis, 1970; Steiner,1977), with a range of clay minerals, from smectite, through mixed-layer clays to chlorite and illite (Harvey and Browne, 1991).

The empirical CO_2 geothermometer of Arnórsson and Gunnlaugsson (1985) was developed to determine the temperature of deep reservoir fluids from fumarole CO_2 concentrations. The method assumes adiabatic boiling of fluid from the deep temperature to local atmospheric pressure. By assuming adiabatic boiling, the original ratio of CO_2/water ratio in the deep fluids can be inferred from the CO_2/steam ratio measured in fumarole steam samples; deep reservoir fluids of a specific temperature boil to local atmospheric pressure with a known mass fraction of steam, giving a predictable CO_2/steam ratio to the fumarole vapour sample (Arnórsson and Gunnlaugsson, 1985).

Contrary to the assumption of adiabatic conditions, it is possible that secondary boiling processes occur, or condensation of steam may occur within the fumarole conduit. In these cases, the geothermometer may be invalid. It follows that Arnórsson and Gunnlaugsson (1985) had suitable fumaroles (i.e. with an adiabatic connection to the reservoir) to develop their geothermometer, as they reported agreement between temperatures inferred from fumaroles, and measured reservoir temperatures from nearby geothermal wells.

It has also been postulated that a fraction of the rising magmatic CO_2 may bypass the geothermal reservoir completely (Werner and Cardellini, 2006). In this situation, CO_2 flux measured the surface would not relate to the reservoir temperature. This situation would not apply to measurements collected on areas of steam heated ground that are known to be supplied by vapour originating from the reservoir (i.e. this study). Alternatively, very large inflows of magmatic CO_2 (rising from beneath) might exceed the capacity of mineral buffers within the reservoir. This would be expected to cause a non-equilibrium, physical control over the concentration of reservoir CO_2, and a high flux of CO_2 at the surface.

In this paper, the geothermometer of Arnórsson and Gunnlaugsson (1985) is applied to abundant CO_2 flux and shallow temperatures measurements made on steaming thermal ground. CO_2 flux and shallow temperatures measurements replace the scarce fumarole samples for which the geothermometer was originally intended. We compare the geothermometry results with deep reservoir temperatures (measured and inferred) from the study areas.

Of the New Zealand systems (Tauhara, Wairakei, Rotokawa, Reporoa and Ohaaki), five are situated within an ~100km^2 area of the TVZ, one of the most productive areas of Quaternary silicic volcanism in the world (Figure 1). The TVZ contains 23 high temperature geothermal systems that have been widely explored by deep drilling and utilized for electricity generation (Rowland and Sibson, 2004; Wilson and Rowland, 2016). At Wairakei, exploitation caused a pressure response in the Tauhara reservoir (located ~10km southeast), which demonstrated a hydrological connection between the two systems. Conversely, the Rotokawa system (10 km to the northeast), has not shown a response to the exploitation of Wairakei (Bixley et al., 2009). The Reporoa geothermal field (Figure 1) was previously thought to be an outflow from Waiotapu, based upon shallow-penetrating resistivity data and geochemical data (Hatherton et al., 1966; Healy and Hochstein, 1973). However, the outflow theory was later refuted based on shallow (Bibby et al., 1994) and deep (Risk et al., 1994) resistivity surveying.

All five systems in the TVZ are recharged by meteoric water (minor magmatic water component), are not presently associated with active volcanism, and are situated at relatively low elevation compared to the surrounding topography (Rissmann et al., 2012; Bloomberg et al., 2014; Harvey et al., 2015a). In these systems, CO_2 flux and shallow temperature measurements were made on areas of bare and vegetated thermal ground (Table 1).

White Island is an active andesitic stratovolcano located ~130 km NE of the other TVZ systems. CO_2 flux and soil temperature measurements were collected from an area of bare thermal ground with high temperature fumaroles on the crater floor (>220°C), and next to a boiling acid lake which is the current location of volcanic activity (Table 1)(Bloomberg et al., 2014).

Copahue is an active stratovolcano in Patagonia, Argentina. CO_2 flux and shallow temperature measurements were made on wet, peaty soils and bare thermal ground in four separate areas on the north-eastern flank of the volcano (Table 1)(Chiodini et al., 2015).

Reykjanes is a coastal geothermal system located on the Reykjanes peninsula, Iceland. The Reykjanes system produces basalt, which is common to all mid-Atlantic ridge volcanism. Surface manifestations at Reykjanes include steam heated ground, fumaroles and mud pools (Table 1)(Fridriksson et al., 2006).

In this study, geothermal systems were selected on the basis that the reservoir temperature was known from deep drilling, or could be inferred by other methods. The objective is to determine if the proposed geothermometer is able to estimate deep reservoir temperature, and so avoid the problems of limited sample size and atmospheric contamination that affect other geothermometers (described above). Table 1 gives summary information relating to the chemical and physical characteristics of the included systems, and references for further information.
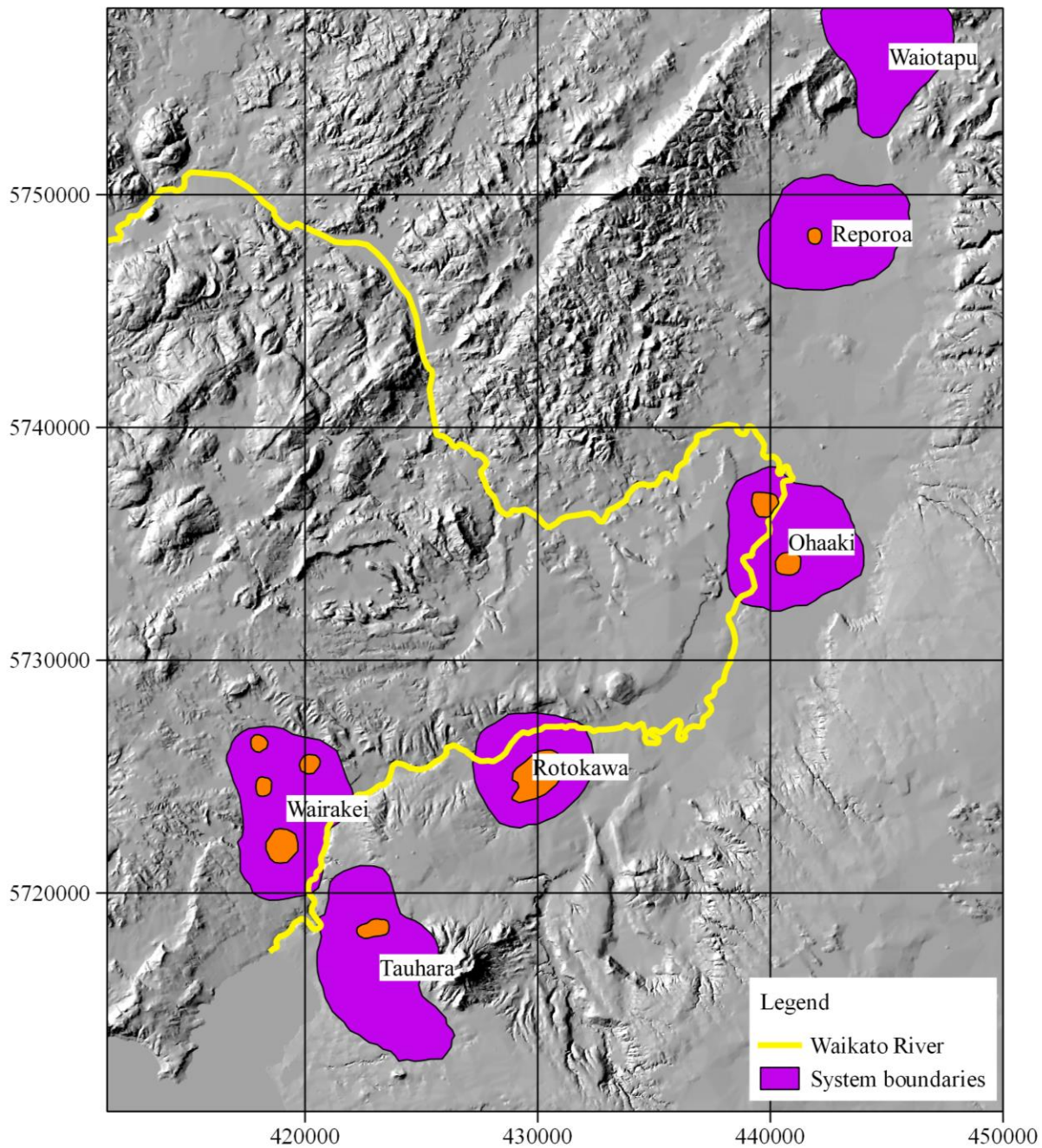
Figure 1: Location of study areas in the Taupō Volcanic Zone overlaid on a satellite digital terrain model (WGS84). System boundaries are based on shallow electrical resistivity data (Bibby et al., 1994). Survey areas (orange) are shown within system boundaries: (a) Hot Hill, (b) Upper Waiora Valley, (c) Geyser Valley, (d) Karapiti, (e) Ohaaki West, and (f) Ohaaki East.

Table 1: System Setting

System	Aquifer Temp[a] (°C)	Host Rock Type[b]	Reservoir Characteristics[c]	Backgr. CO2 flux (g m^{-2} d^{-1})[d]	Exploited System[e]	Reference
Wairakei, New Zealand	240-250	Andesite-Rhyolite	Low-gas, non-magmatic, neutral.	5	yes	(Giggenbach, 1995; Werner et al., 2004; Glover and Mroczek, 2009; Rosenberg et al., 2009)
Tauhara, New Zealand	250-270	"	Low-gas, non-magmatic, neutral.	10	yes	(Giggenbach, 1995; Glover and Mroczek, 2009; Rosenberg et al., 2009; Rosenberg et al., 2010)
Rotokawa, New Zealand	<300 (intermediate) 300-340 (deep)	"	High-gas, possible magmatic conditions at depth in south of field. Neutral at depth.	5	yes	(Giggenbach, 1995; Bloomberg et al., 2014; McNamara et al., 2016)
Ohaaki West, New Zealand	180-310	"	High-gas, non-magmatic.	15	yes	(Giggenbach, 1995; Rissmann et al., 2012)
Ohaaki East, New Zealand	240-290	"	High-gas, possible magmatic conditions at depth. Neutral.	15	yes	(Giggenbach, 1989; Giggenbach, 1995; Christenson et al., 2002; Rissmann et al., 2012)
Reporoa, New Zealand	unknown	"	Unknown.	10	no	(Healy, 1973; Simpson and Bignall, 2016)
White Island, New Zealand	high	Andesite	High gas, near surface magmatic conditions. Active volcano.	0	no	(Giggenbach, 1987; Houghton and Nairn, 1991; Hedenquist et al., 1993; Giggenbach et al., 2003)
Copahue, Argentina	240-300	Basalt-Andesite	Unknown, but Magmatic conditions nearby (~6km). Active volcano.	5-26	no	(Agusto et al., 2013; Chiodini et al., 2015)
Reykjanes, Iceland	290	Basalt	Low gas, near-neutral.	4	yes	(Arnórsson, 1978; Fridriksson et al., 2006; Freedman et al., 2009; Ármannsson, 2016)

[a] Temperature from deep well measurements (White Island is inferred)
[b] From deep well cuttings and core
[c] From surface and sub-surface observations
[d] Background biological CO2 flux estimated using statistical methods (Copahue, Reykjanes) (Chiodini et al., 1998), or ^{13}CO2 isotope analysis (New Zealand systems) (Harvey et al., 2015a; Harvey et al., 2015b)
[e] Hydrothermal reservoir is utilized for power generation

2. METHODS

2.1 CO2 Flux Measurement Methods

All soil CO_2 flux measurements were made with a West System's accumulation chamber meter, an established method for quantification of soil CO_2 flux in volcanic and geothermal areas (Brombach et al., 2001; Chiodini et al., 2005; Fridriksson et al., 2006; Hernández et al., 2012; Rissmann et al., 2012). The method quantifies CO_2 flux using a ~200mm diameter chamber, which is placed on the soil surface to obtain a seal. The increase in CO_2 concentration in the chamber over time is recorded; the rate of concentration increase in CO_2 is proportional to the flux (mmol m^{-2} d^{-1}).

2.2 Method for Measurement of Heat Flux from Steaming Ground: Wairakei, Tauhara and Reporoa

In each location that CO_2 flux was measured, soil temperatures were also recorded with a handheld temperature probe inserted to ≤ 1 m below ground level. Temperature measurement were made at 5-10 cm intervals, depending on the temperature gradient. In locations with very high heat flow, temperatures were recorded at 5 cm intervals so the boiling point depth could be established with more accuracy (for pure water at local elevation).

Heat flux was derived from the shallow temperature measurements using the empirical method of Hochstein and Bromley (2005). Their method provides total heat flux per m2, as the sum of convective and conductive vapour fluxes:

$$Qtot = \alpha \, (Zbp/Zo)^{-\beta} \qquad (1)$$

Where Qtot is the total heat flux (W m^2), Zbp is the depth to boiling, α (185W m^2) and β (0.757) are empirically derived constants, and Zo is the unit for depth (1 m). If boiling was not reached at 1 m depth, it was estimated by extrapolation assuming a polynomial or power law relationship (whichever curve gave the best fit). Measurements with Zbp > 2 m were excluded to limit error from the extrapolation.

2.3 Method for Measurement of Heat Flux from Steaming Ground: Ohaaki, Rotokawa, White Island, Copahue and Reykjanes

Shallow temperature data from these areas were collected at a single depth (0.15 m), except Copahue (0.1 m). Details of the methods used for shallow temperature measurement in these areas is given in references (Table 1). This method does not give multi-measurement temperature profiles (as for Tauhara, Wairakei and Reporoa). However, measurements from these areas could be input to Equation 1 using the relation between depth to boiling point, and temperature at 0.1 m and 0.15 m. This relation was determined by regressing depth to boiling point depth on temperature at 0.15 and 0.10 m using profiles from Wairakei, Tauhara and Reporoa (n = 511)(Figure 2a and Figure 2c).

The regression uncertainty (scatter) increases with boiling point depth (Figure 2a and Figure 2c). At 2 m boiling point depth, the corresponding temperature at 0.15 m (23°C)(Figure 2a) is equivalent to the ambient summer temperatures at Wairakei, Tauhara and Reporoa (daytime). Accordingly, only measurements with a derived depth to boiling point of <2 m were included.

To quantify uncertainty for different ranges of shallow temperature, we separated the Tauhara, Wairakei and Reporoa datasets into 5 °C intervals (between 40 – 100 °C), then linear regressed each interval. Temperature interval was plotted against standard error (SE) (Figure 2b and Figure 2d).
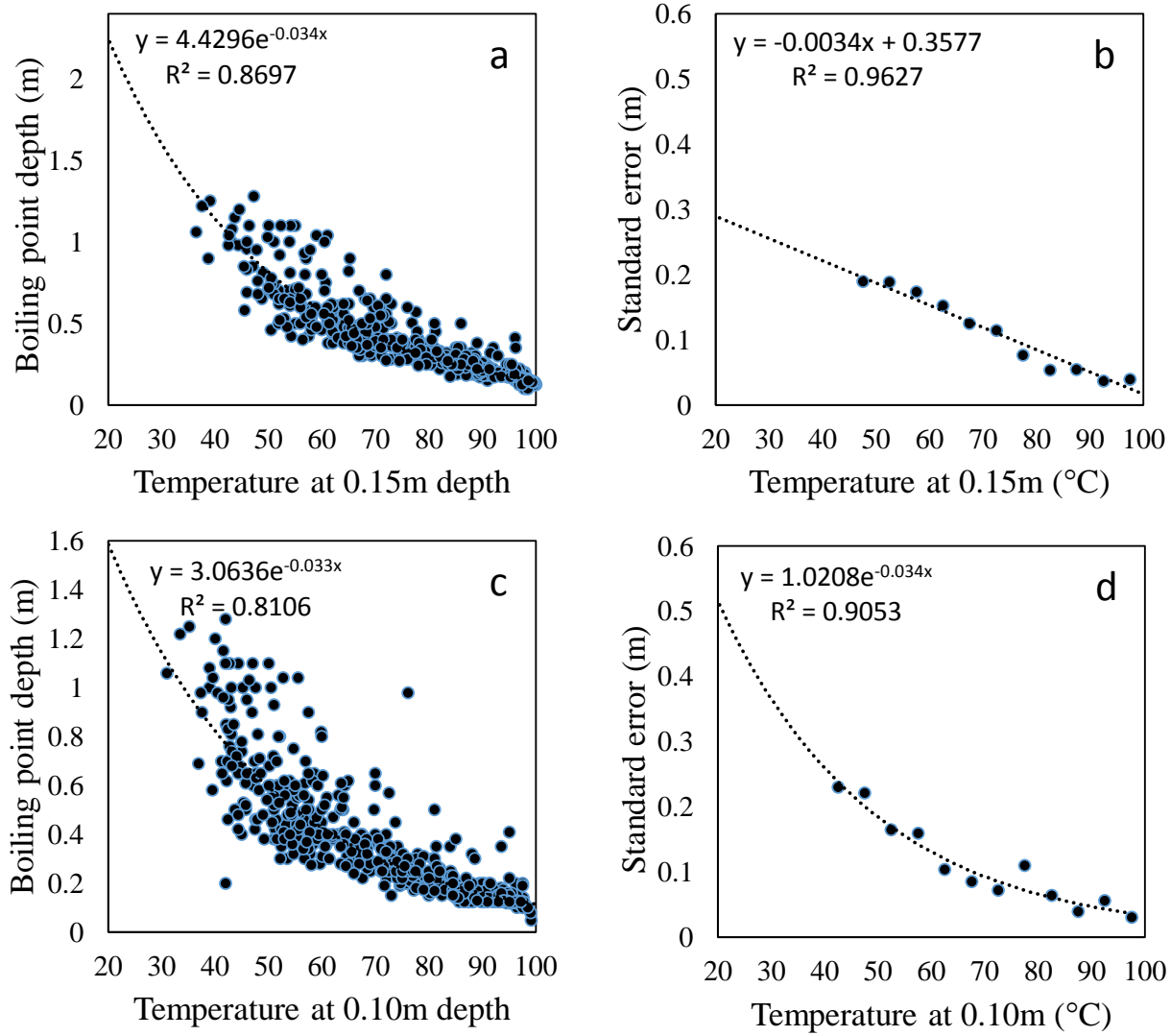
Figure 2: Depth-to-boiling point versus temperature at 0.15 m (a), and 0.1 m depth (c). Note: scatter decreases as shallow temperature increases. Scatter (standard error) versus depth for (a) and (c) is plotted in (b) and (d), respectively.

2.4 Method for Inference of Steam Flux

Steam flux can be inferred from Equation (1) by assuming heat flux results from the sum of i) convective steam flux and ii) steam condensation in the shallow sub-surface of the soil (conductive heat flux) (Brombach et al., 2001; Werner et al., 2004; Hochstein and Bromley, 2005; Fridriksson et al., 2006):

$$Fstm = Qtot \ (hs - hw)^{-1} \tag{2}$$

Where Qtot is the inferred heat flux (Equation 1), Fstm is the steam flux (kg m^2 s^{-1}), hs, is the enthalpy of steam at local boiling point (kJ kg^{-1}), and hw is the enthalpy of water in the liquid phase at ambient conditions (kJ kg^{-1}).

2.5 Method for Determination of Deep Reservoir Temperature from CO2/H2O

The concentration of CO_2 in steam supplying the thermal area can be derived from the ratio of CO_2 flux and steam flux (see above methods). This approach was previously applied, and gave results comparable to concentrations derived from fumarole gas analysis (Brombach et al., 2001; Werner et al., 2004). Concentrations derived in this way may be converted to temperature (°C) using the CO_2 geothermometer of Arnórsson and Gunnlaugsson (1985):

$$TCO_2 \ Flux = -44.1 + 269.25R - 76.88R^2 + 9.52R^3 \tag{3}$$

Where R is the logarithm of the concentration of CO_2 in steam supplying the thermal area (log mmol kg^{-1}, from Equation 2 and CO_2 flux measurements) and TCO2 Flux is the temperature of the reservoir (°C). Equation 3 may be applied to geothermal reservoirs hosted in

mafic to silicic rocks with high temperature (Arnórsson and Gunnlaugsson, 1985), which includes all of the geothermal systems in this study (Table 1 and Table 2).

Alternatively, the CO2 geothermometer of Giggenbach (1984)(his Equation 15) may be adapted in the same way (assuming adiabatic boiling from equilibrium reservoir temperature to atmospheric pressure; Arnórsson and Gunnlaugsson, 1985):

$$\text{TCO2 Flux Gigg (°C)} = 51.773R + 154.04 \qquad (4)$$

Where R is the logarithm of the concentration of CO2 in steam supplying the thermal area (log mmol kg^{-1}, from Equation 2 and CO2 flux measurements) and TCO2 Flux Gigg is the temperature of the reservoir (°C).

TCO2 Flux (Equation 3) and TCO2 Flux Gigg (Equation 4) were compared for a range of simulated CO2 concentrations (Figure 3). Results show Equation 4 provides lower temperatures at high CO2 concentrations, and higher temperature estimates at lower CO2 concentrations. Results from both equations are similar (<10°C difference) between 200-300°C (Figure 3).

In this paper we have utilised Equation 3 because it was originally intended to estimate deep reservoir temperatures from CO2 concentration in fumarole steam. The application of Equation 3 to a population of survey measurements (i.e. an area of steaming ground) transforms the lognormal raw data into a normally distributed population of reservoir temperatures. This population can then be described by normal statistics (mean, mode and standard deviation).

For White Island, Ohaaki, Rotokawa, Reykjanes, and Copahue, depth to boiling point (Equation 1) was estimated by regression (Figure 2). The regression scatter and its effect on the final reservoir temperature estimate was examined using a Monte Carlo simulation developed in Microsoft Excel (1000 realisations)(Robert and Casella, 2013); in the simulation a boiling point depth was created for each shallow temperature measurement by random selection from a normally distributed population; actual data was used to model the normal distribution; the population mean was set to the depth to boiling point estimated from the regression (Figure 2a and Figure 2c). The standard deviation was set to the standard error at that temperature (Figure 2b and Figure 2d).
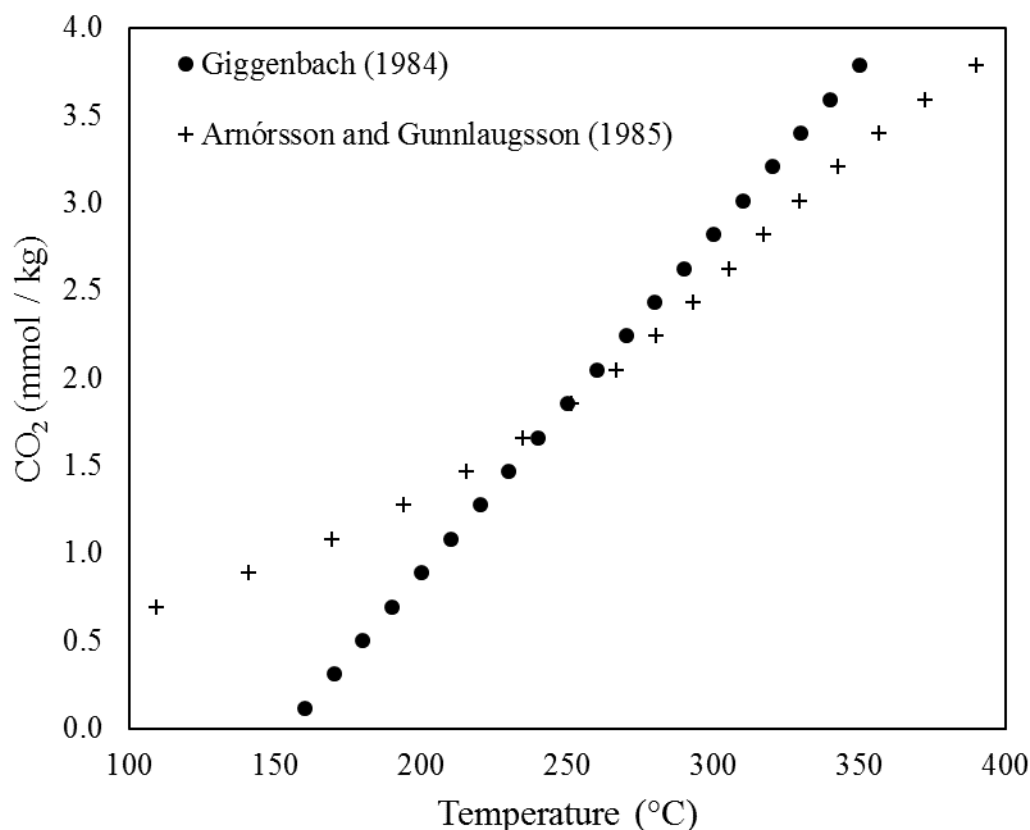

Figure 3: Comparison of TCO2 Flux (Arnórsson and Gunnlaugsson, 1985; Equation 3) and TCO2 Flux Gigg (Giggenbach, 1984; Equation 4) for a range of CO2 concentrations in surface vapour.

Harvey et al.

2.6 Determination of Biological Background CO2 Flux

It was unavoidable that a number of CO2 flux measurements were collected in areas where biological (i.e background non-magmatic) CO2 flux was expected. The magnitude of biological CO2 flux in these areas was previously estimated using statistical techniques (Copahue, Reykjanes)(Fridriksson et al., 2006; Chiodini et al., 2015), and 13CO2 isotope analysis for the New Zealand systems (Harvey et al., 2015b)(Table 1). The estimated contribution from biological flux was subtracted from measurements prior to the TCO2 Flux calculation. CO2 flux values that became negative after subtraction were disregarded.

3. RESULTS

Shallow temperature and soil CO2 flux results were converted to TCO2 Flux (°C)(Equation 3), plotted as histograms (Figure 4 - Figure 7), and summarised in Table 2. The summary statistics derive from 4274 measurements; eight systems in New Zealand, Argentina and Iceland. Mean TCO2 Flux temperatures range from a low of 222 °C at the Wairakei outflow to 314 °C at Reporoa. Histogram peak (mode) temperatures range from 230 °C at the Wairakei outflow to 320 °C at White Island.

For White Island, Rotokawa, Ohaaki, Copahue and Reykjanes, depth to boiling point (Equation 1) was estimated by regression (Figure 2). The effect of scatter of the regression on mean TCO2 Flux was examined by Monte Carlo simulation. For Copahue, the simulation was within 4 °C of the actual data. For White Island, Rotokawa, Ohaaki, and Reykjanes, the simulation gave mean TCO2 Flux within 1 °C of the mean TCO2 Flux of the actual data.

Table 2: Summary of Results

Area	n^a	Survey Area (m^2)	CO2/H2O^b (mmol/100 mol)	CO2/H2O^b (log mmol/kg)	Mean $T_{CO2\ Flux}$ ^{c} (°C)	±^{d} (°C)	Mode(s) $T_{CO2\ Flux}$ ^{e} (°C)	Fig.
Tauhara	332	1.4E+05	219	2.09	266	71	270	Fig. 5
Wairakei Outflow Areas	263	3.2E+05	70	1.59	222	92	190, 230	Fig. 4
Wairakei Upflow Areas	148	2.0E+05	135	1.88	249	83	270	Fig. 4
Reporoa	104	2.3E+03	1027	2.76	314	97	290-330	Fig. 5
Rotokawa	1186	1.7E+06	693	2.59	304	158	280, 320	Fig. 5
Ohaaki West	417	2.1E+05	308	2.23	272	96	190, 260, 300	Fig. 6
Ohaaki East	386	3.4E+05	446	2.39	287	96	280	Fig. 6
White Island	581	2.8E+05	741	2.61	303	129	320	Fig. 6
Copahue	447	9.8E+05	547	2.48	293	133	300	Fig. 6
Reykjanes 2004	167	1.50E+05	310	2.24	276	96	270	Fig. 7
Reykjanes 2007	243	2.40E+05	233	2.11	267	80	290	Fig. 7
All data 2004 & 2007	410		272	2.16	271	86	280	Fig. 7

[a]Number of measurements in survey area

[b]CO2/H2O ratio corresponding to the mean temperature

[c]Arithmatic mean of temperatures

[d]two standard deviations

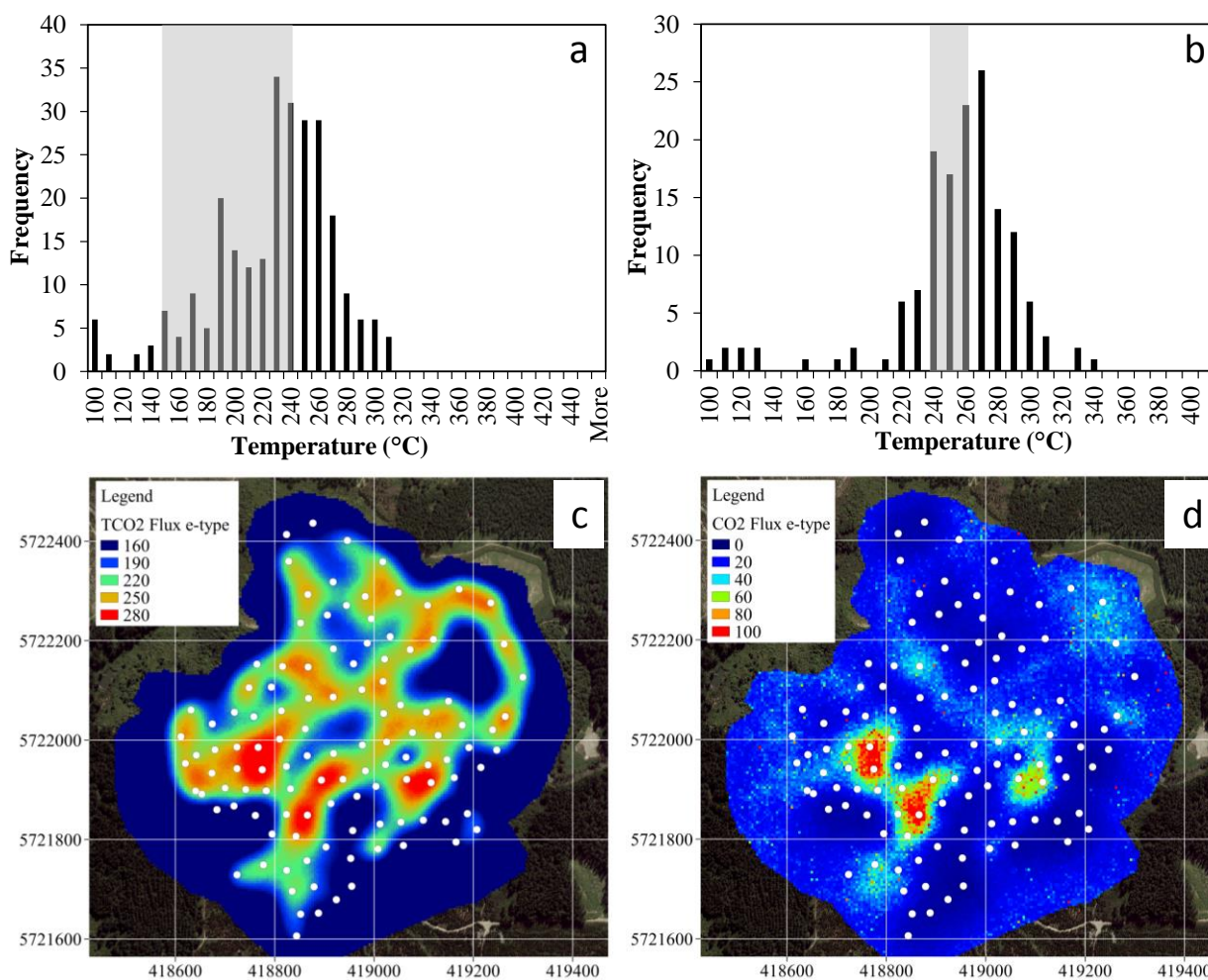[e]Temperature from histogram peak(s)

Figure 4: TCO2 Flux histograms for (a) Wairakei outflow areas (Karapiti and Geyser Valley), and (b) Wairakei upflow areas (Waiora Valley and Hot Hill). Shaded area shows range of measured temperatures from deep wells (Table 3). Interpolation (Sequential Gaussian Simulation) at Karapiti for (c) TCO2 Flux (°C), and (d) CO2 Flux (g m^{-2} d^{-1}). White points show measurement locations. Note: agreement between spatial distribution of TCO2 Flux (c) and CO2 flux (d).
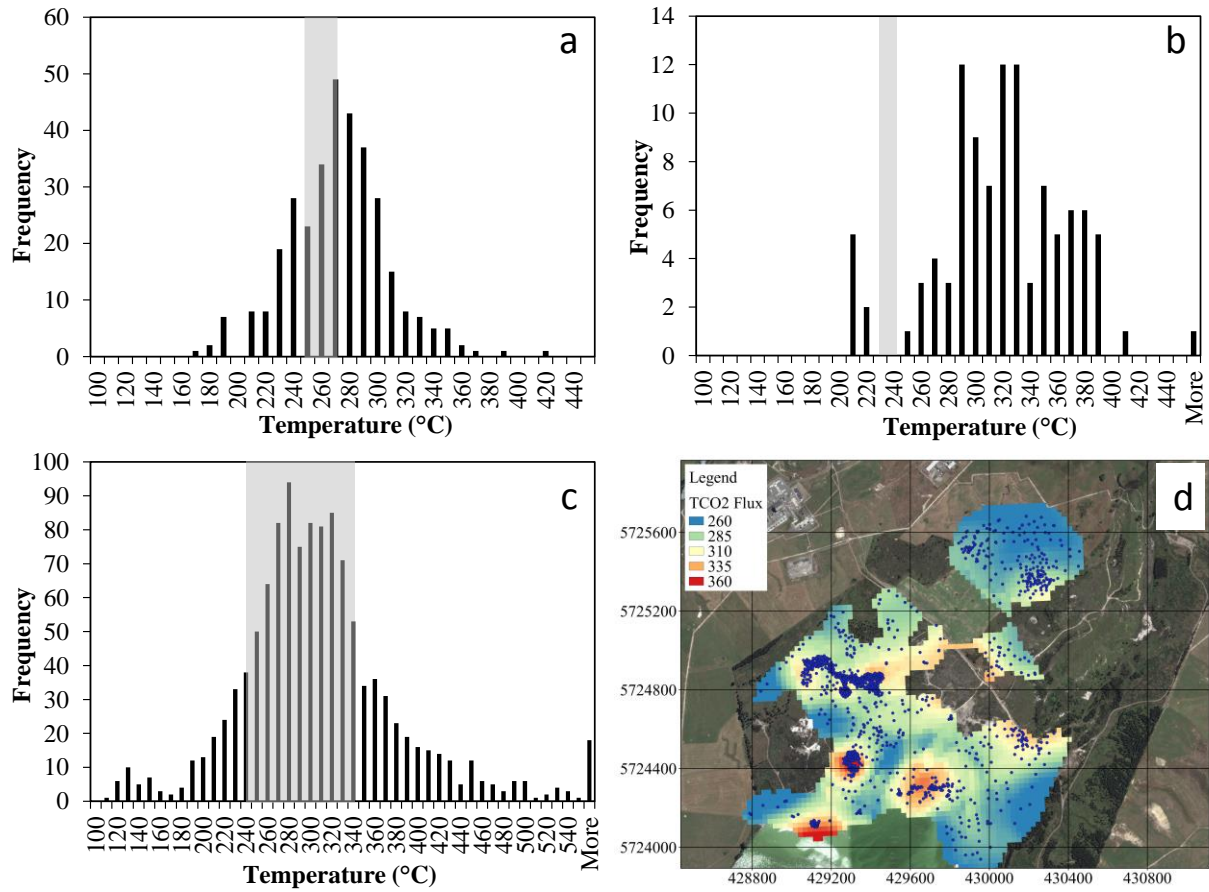
Figure 5: **TCO2 Flux histograms for (a) Tauhara (Pony Club), and (b) Reporoa (Opaheke), (c) Rotokawa, and (d) spatial distribution for Rotokawa (°C): blue points show measurement locations. Shaded area shows range of measured temperatures from deep wells (Table 3). Note: TCO2 Flux reaches maximum near Lake Rotokawa (south of map) and decreases to north (interpolation by Ordinary Kriging).**
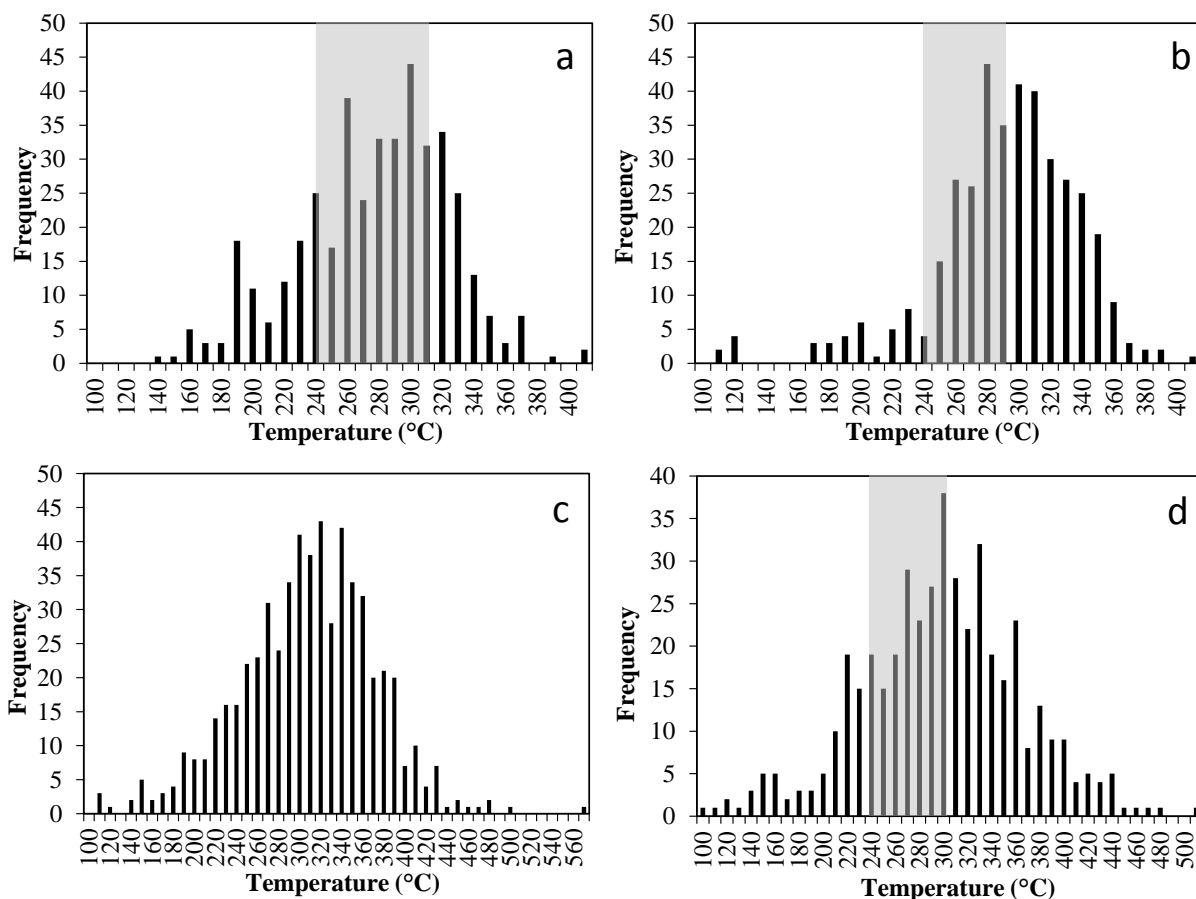
Figure 6: TCO2 Flux histograms for (a) Ohaaki West, and (b) Ohaaki East, (c) White Island and (d) Copahue (all areas). Shaded area shows range of measured temperatures from deep wells (Note: most feed-zones at Ohaaki West exceed 240°C)(Table 3)
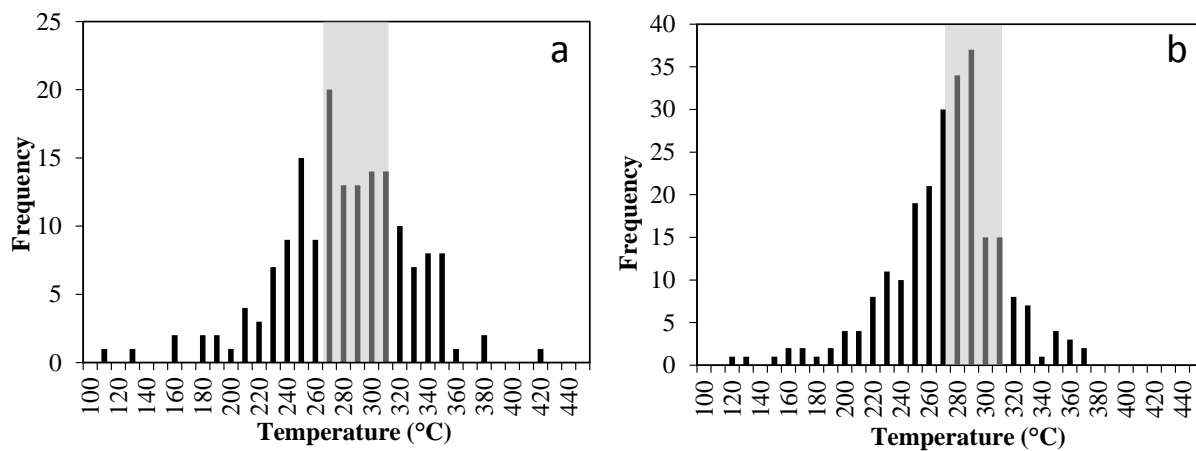
.

Figure 7: TCO2 Flux histograms for Reykjanes (a) 2004, and (b) 2007. Shaded area shows range of measured temperatures from deep wells (Table 3).
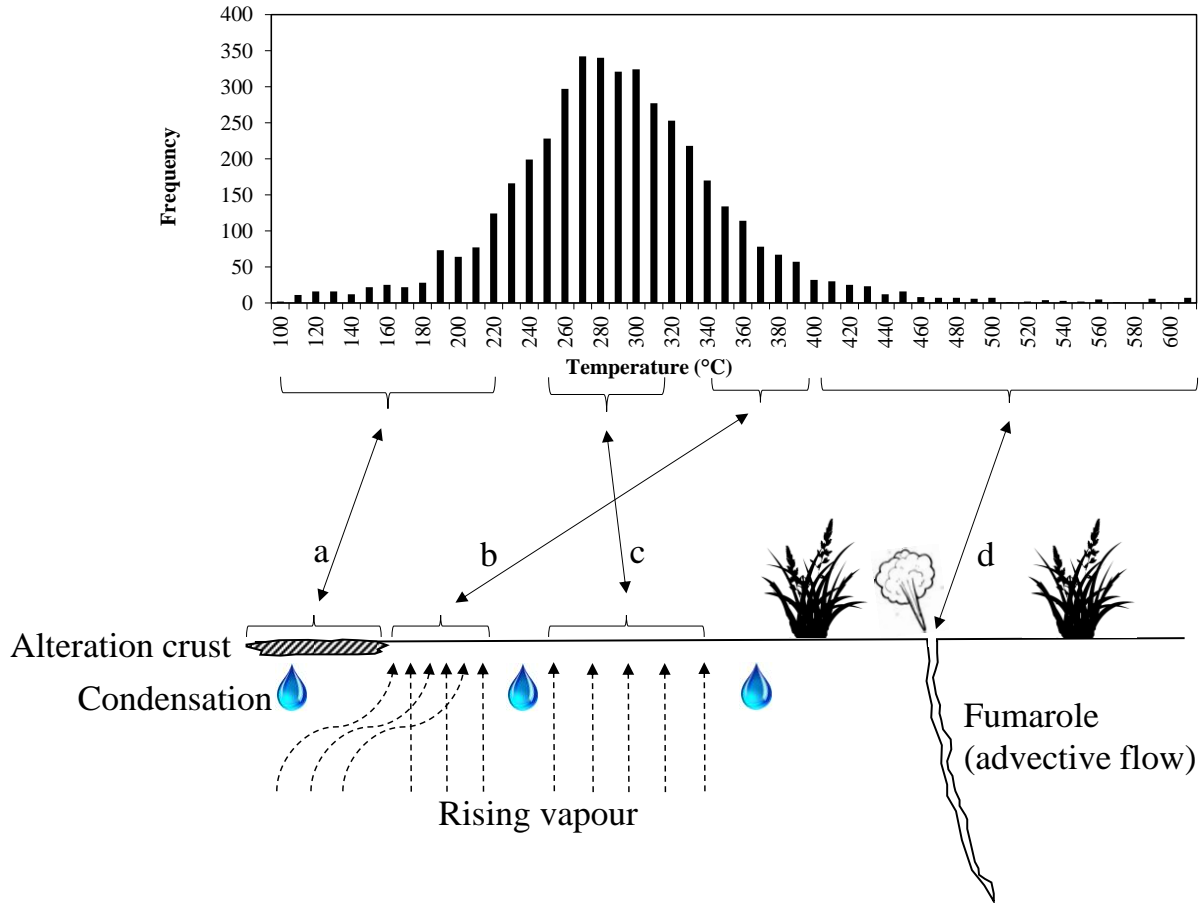
Figure 8: Causes of variability of TCO2 Flux within a thermal area. (a) Rising vapour encounters a near surface impermeable layer (e.g. alteration crust), (b) re-routed CO2 converges with adjacent vapor stream and enters the atmosphere. This creates localized areas of anomalously high CO2 flux, (c) composition of vapour reflects adiabatic boiling of the reservoir, and (d) very high CO2 fluxes and correspondingly high TCO2 Flux are expected where vapour flows advectively from the system.

4. DISCUSSION

Here we compare deep reservoir temperatures measured in geothermal wells to temperatures estimated from TCO2 Flux (Table 3). The aim is to show the geothermometers reliability. In addition, the accuracy of estimates of H2O flux and the variability of TCO2 Flux are considered.

Table 3: Aquifer Temperatures versus CO2 flux geothermometer temperatures

System	Aquifer Temp (°C)[a]	$T_{CO2\ Flux}$ (°C)[b]		Notes
		Mean	Mode(s)	
Tauhara	250-270	266	270	Deep aquifer temperatures in the survey area based on deep well data (Rosenberg et al., 2010).
Wairakei Outflow Areas	150-240	222	190, 230	Deep aquifer temperature from deep well data (Glover et al. 2001; Bixley et al., 2009; Sepulveda et al., 2012).
Wairakei Upflow Areas	240-260	249	270	
Reporoa	234	314	290-330	Deep aquifer is thought to have high CO2 based on one exploration well (RP1)(DSIR, 1967).
Rotokawa	240-300 (intermediate), 300-340 (deep)	304	280, 320	Deep and intermediate aquifer temperatures (Winick et al., 2009 and McNamara et al., 2016).
Ohaaki West	180-310	272	190, 260, 300	Measured temperatures from deep wells at major and secondary feed zones (Mroczek et al., 2016). The deep aquifer at Ohaaki is generally reported to be 300-310 °C (Mroczek et al., 2016; Rissmann et al., 2012; Hedenquist, 1990).
Ohaaki East	240-290	287	280	
White Island	High	303	320	Vapour core system (Giggenbach, 1987)
Copahue	240-300	293	300	Deep aquifer temperature from deep wells located 1–2 km from the survey areas (240-260 °C)(Chiodini et al., 2015), and gas geothermometry from fumaroles in the survey areas (250-300°C)(Agusto et al., 2013).
Reykjanes (2004)	275-310	276	270	Deep aquifer temperature from deep wells in the survey area [Fig 2(b), Freedman et al.(2009)].
Reykjanes (2007)	275-310	267	290	

[a]Temperature from deep well measurements

[b]Temperature from CO2 flux geothermometer (mean and mode)

4.1 Tauhara and Wairakei

The temperature of the Wairakei outflow was taken from bore holes located outside of Te Mihi. Te Mihi is located between the Hot Hill and Upper Wairoa Valley survey areas (Fig.1a - b), and is considered to be the main upflow (Bixley et al., 2009). Temperatures in outflow areas vary (150-240 °C), and increase near Te Mihi (Bixley et al., 2009). This range agrees with the mean of CO2 flux geothermometer data in this area (μ=222 °C)(Table 3). The distribution of Wairakei outflow TCO2 Flux values (Karapiti and Geyser Valley; Fig.1c - d) show major (230 °C) and minor (190 °C) histogram peaks (Figure 4a). This may indicate separate aquifers are supplying CO2 and steam in the outflow areas, particularly Karapiti.

It was noted in previous studies that gas and steam discharging at Karapiti originate from the Wairakei upflow zones (Glover et al., 2001; Allis, 1981); lateral fluid flow occurs along fractures in the shallow upper surface of the Karapiti Rhyolite toward Karapiti (Allis, 1981). Deep geothermal bores in the vicinity of Karapiti are relativel cool (<200 °C)(Allis, 1981). It follows that the presence of two peaks in our data may correspond to a deeper, cooler aquifer directly beneath Karapiti (minor peak), and the main upflow that is located near Te Mihi (major peak).

The Wairakei upflow zone temperature was interpreted from bores located at Te Mihi, which have remained steady (240-265 °C) since 1993 (Glover et al., 2001; Bixley et al., 2009). This range is close to the mean (μ=249 °C), and mode (270 °C) of TCO2 Flux for Wairakei upflow data (Upper Waiora Valley and Hot Hill; Fig.1a - b)(Figure 4b)(Table 3).

Harvey et al.

At Karapiti, mapped TCO2 Flux (Figure 4c) and CO2 flux (Figure 4d) show good agreement. This suggests that CO2 flux dominates H2O flux in the TCO2 Flux calculation. This can be explained because H2O flux varies by ~1 order-of-magnitude, whereas CO2 flux varies by 3-4 orders-of-magnitude (for our dataset). The single order-of-magnitude variation of diffuse H2O flux at Karapiti is in agreement with an earlier report at Karapiti (Hochstein and Bromley, 2005) and another study at Solfatara (Italy)(Werner et al., 2006). By comparison, the range of CO2 flux measurements is much wider, and this has been noted in numerous studies previously (e.g. Fridriksson et al., 2006; Werner and Cardellini, 2006; Bloomberg et al., 2012; Rissmann et al., 2012).

At Tauhara, the deep temperature is taken to be the average measured temperature from bores located either side of the study area (TH1, 248 °C and TH3, 272 °C). Neither bore has shown a temperature change since the 1970's (Rosenberg et al., 2010). The average temperature of these bores (260 °C) is close to the mean and mode TCO2 Flux (266 and 270 °C, respectively)(Figure 5a, Table 3).

A t-test (independent samples) between TCO2 Flux populations at Wairakei (μ=249°C), and Tauhara (μ=266°C) was found to be statistically significant ($p<0.05$). This result is consistent with the observed higher bore temperatures at Tauhara (Table 3), and with previous reports that Tauhara has a separate, higher temperature upflow than Wairakei (280-300°C)(Rosenberg et al., 2010).

4.2 Rotokawa

Data from bore holes shows chemical gradients from Rotokawa North (Waikato River) to Rotokawa South (Lake Rotokawa), with higher concentrations of B, Li, Cl, Cs and CO2 in the south. B/Cl and CO2/Cl ratios are also greater in the south. The geochemical data and chloride-enthalpy mixing trends suggests a main upflow in beneath Lake Rotokawa in the south of the field (Giggenbach, 1995; Winick et al., 2009; McNamara et al., 2016).

Well data identifies distinct intermediate (<300 °C) and deep aquifers (300-340 °C), which are separated by a smectite clay zone. The distribution of TCO2 Flux at Rotokawa has peaks at 280 °C and 320 °C (Figure 5c)(Table 3) that may correspond to the intermediate and deep aquifers. Spatially, TCO2 Flux shows higher temperatures near Lake Rotokawa (Figure 5d), consistent with the existence of the main upflow in this area. The Rotokawa population (μ=304°C) has the largest standard deviation of all areas (2 standard deviations = 158 °C), which results from the wide temperature gradient between the north of the survey area and Lake Rotokawa.

4.3 Ohaaki

Bore data shows Ohaaki East and West reservoir fluids have distinct chemical characteristics, and may have separate upflows. Previous studies concluded the East Bank is more "magmatic" based on higher CO2, and higher B/Cl ratios in the fluid (Giggenbach, 1989; Christenson et al., 2002; Rissmann et al., 2012); further, that the East Bank's chemistry results from a younger and shallower heat source (i.e. relative to the West bank)(Christenson et al., 2002). Another explanation for the distinctive geochemistry is that a single deep parent fluid diverges to the East and West, then undergoes secondary boiling (boiling of a shallow, CO2-rich, steam-heated aquifer) and dilution processes (Hedenquist, 1990, Mroczek et al., 2016).

Bore data from secondary and major feed-zones shows temperatures range from 240-290 °C on the East Bank, and 180-310 °C on the West Bank, increasing with depth (Mroczek et al. 2016)(Table 3). The distribution of TCO2 Flux at Ohaaki East (Figure 1f) is unimodal (280 °C, Figure 6b), which may reflect the narrow range of feed zone temperatures (240-290 °C)(Mroczek et al. 2016). The distribution of TCO2 Flux at Ohaaki West (Figure 1e) is tri-modal, with peaks at 190 °C, 260°C, and a dominant peak at 300 °C (Figure 6a), which may reflect the wider range of feed temperatures (180-310 °C). At Ohaaki West, most feed zones exceed 240°C (Mroczek et al. 2016 – see Figure 6 in that study).

A t-test (independent samples) was undertaken to compare the population of TCO2 Flux values at Ohaaki East (μ=287 °C) to those at Ohaaki West (μ=272 °C). The test result was statistically significant ($p<0.05$). The higher TCO2 Flux at Ohaaki East is consistent with previous observations of higher CO2, and the more magmatic character for eastern fluids (Giggenbach, 1989; Christenson et al., 2002; Rissmann et al., 2012).

4.4 Reporoa

There is only one deep bore at Reporoa (RP-1), which is located approximately 100m from the study area. RP-1 temperatures were measured shortly after drilling and peaked at 234 °C (975 mMD)(Healy, 1973). However, the well discharged for less than 6 hours and was probably diluted/cooled by drilling fluids (Simpson and Bignall, 2016).

The bore fluids were lower in chloride and lithium than surface waters from nearby hot springs at Opaheke (Simpson and Bignall, 2016; DSIR, 1967), which also suggests dilution. It follows that reservoir temperatures beneath the Reporoa survey area are probably hotter than measured at RP-1. The peak of the TCO2 Flux histogram at Reporoa is poorly formed, but an emergent peak (290-330°C, Figure 5b), and high mean TCO2 Flux (μ=314 °C) indicates temperatures at depth may be considerably hotter than those measured in RP-1. Reporoa has the smallest population (n=104) of all areas, which causes the histogram to be poorly developed.

4.5 White Island

White Island is an active volcano, inferred to host an acidic liquid geothermal reservoir surrounding a vapour-core at depth (Houghton and Nairn, 1991). It has no deep wells.

The TCO2 Flux histogram for White Island is unimodal (320 °C, Figure 6c), the highest temperature in this study. At White Island, strong magmatic CO2 flux would penetrate or bypass the acidic liquid reservoir, especially during eruptive events. Such a process would invalidate the TCO2 Flux geothermometer, which assumes temperature dependent mineral-water equilibrium in neutral pH fluids. White Island is included in this study as it provides an indication of how TCO2 Flux behaves in an acid-magmatic environment.

4.6 Copahue

Deep bores located 1–2 km from the survey indicate aquifer temperatures (240-300 °C)(Chiodini et al., 2015), similar to gas geothermometry from fumaroles located in the survey areas (250-300 °C)(Agusto et al., 2013)(Table 3). Copahue is an active volcano with an acid crater lake located ~6 km from the survey areas.

The TCO2 Flux histogram at Copahue is unimodal (300 °C, Figure 6d), at the top of the range of aquifer temperatures in the survey area based on fumarole geothermometry (240-300 °C).

4.7 Reykjanes

Both 2004 and 2007 TCO2 Flux histograms for Reykjanes are unimodal (270 and 290 °C respectively, Figure 7). The apparent increase in deep reservoir temperature at Reykjanes may relate to an increase in production well enthalpy that occurred over the same period. The enthalpy increase was caused by the onset of fluid extraction (exploitation of the field), with associated boiling and pressure decline. Between 2004 - 2008, production well enthalpy increased from 1210 – 1400 kJ/kg (liquid enthalpy at 275 - 310 °C) to 1450 - 1950 kJ/kg. Surface activity (surface steam and CO2 fluxes) increased rapidly during this period (Fridriksson et al., 2010).

Aquifer temperatures based on wells in the study area range from 275- 310°C (Freedman et al., 2009; Figure 2b in that study)(Table 3), and average ~290 °C (Fridriksson et al., 2006).

4.8 Variability of TCO2 Flux Within the Histogram

Results show CO2 flux and shallow temperature measurements can give an estimate of geothermal reservoir temperature. TCO2 Flux histograms present as normally distributed datasets. All systems in this study (excluding White Island) have liquid-phase reservoirs at depth. In all cases, the temperature range reported for each system is narrower than the range of TCO2 Flux values (Table 1). This indicates the variability in our datasets is determined by random processes occurring i) in the subsurface, and/or ii) measurement error (i.e. rather than by the variability in the reservoir).

It is possible the variability results from surficial "alteration crusts". Thin crusts of fumarolic sublimates and/or alteration, were previously reported to cause highly variable CO2 flux in thermal areas (Chiodini et al., 1996). Impermeable thermal clays and alteration crusts were also noted to effect CO2 flux in this study (Reporoa, Tauhara, and Wairakei thermal areas), and in previous studies at White Island and Rotokawa (Bloomberg et al., 2012). CO2 flux was observed to vary orders of magnitude over very small distances (~1 m) where crust was present. Such surface crusts, or other obstructions, might affect the quantification of H2O and fluxes in different ways, as H2O vapour is subject to condensation at the soil-atmosphere interface (CO2 is not).

For example, consider the low tail of the TCO2 Flux histogram (Figure 4 - Figure 7). Here, measurements are affected by restricted near-surface permeability, which results in low vapour flux; Figure 8a shows the rising vapour (mix of CO2 and H2O in the gas phase) encountering a near surface, impermeable layer. The H2O component of the vapour is blocked, condenses, then releases heat by conduction. Conductive heat loss is detected by the probe, giving a large denominator in the CO2/H2O ratio (low TCO2 Flux). The CO2 is also blocked, but does not condense. Instead, it is channeled to surface elsewhere; the CO2 is not detected by the instrument, which gives a small numerator (low TCO2 Flux).

The same process may contribute to measurements in high tail, as the channeled CO2 combines with an adjacent vapor stream and enters the atmosphere. This process creates focused areas of anomalously high CO2 flux (Figure 8b), which gives a relatively large numerator (high TCO2 Flux).

Very high TCO2 Flux values may be expected for advective CO2 flows (high numerator) (e.g. fumaroles or small vents). These point-sources of CO2 are analogous to including a gold nugget in a bulk metallurgical assay; in geostatistical terms, this is the "pure nugget" effect (Armstrong, 1998). Critically, water vapour may flow to the atmosphere without releasing much heat to the soil (advective heat loss), so there is no nugget in the denominator (Figure 8d).

Shallow temperature measurements were made adjacent to the CO2 flux meter's accumulation chamber, which may not provide an estimate of H2O flux directly beneath the chamber. This provides an alternate mechanism through which high spatial variability can randomly impact our results. The error's magnitude will be a function of the spatial variability of the vapour flux and is part of the nugget effect (Armstrong, 1998). Surveying at higher density (i.e. sub-meter scale measurement spacing) might resolve these effects, but is outside the scope of this investigation.

The processes described above are extreme cases, and may cause the histogram tails. More commonly, we expect the relative proportion of H2O and CO2 in the rising vapour to result from adiabatic boiling of the reservoir at depth (Figure 8c). To summarize, variability shown in the histogram is not caused by variability in reservoir temperature. Rather, it results from spatially variable permeability in near-surface materials.

5. CONCLUSIONS

In this study we have compared geothermometry based on measurements of shallow temperature and CO_2 flux on steaming ground (TCO2 Flux), with measured/inferred reservoir temperatures from eight geothermal areas in New Zealand (6), Argentina (1) and Iceland (1). Survey measurements from steaming ground provided populations of temperatures that were described by normal statistics (mean, mode and standard deviation).

Mean TCO2 Flux estimates fall within the range of measured reservoir temperatures for Rotokawa, Wairakei, Tauhara, Ohaaki, Reykjanes and Copahue. At White Island, powerful CO_2 flows escape the magma, rise, and penetrate the acidic liquid reservoir, especially during eruptions. The TCO2 Flux geothermometer depends on mineral-water equilibrium in neutral reservoir fluids, so would not be reliable at White Island or in similar acid-magmatic settings.

We propose the TCO2 Flux geothermometer gives an estimate of reservoir temperature that can avoid the problems of limited sample size inherent to current gas and water geothermometers. Although we based TCO2 Flux on the geothermometer of Arnórsson and Gunnlaugsson (1985), it would be equally possible to adapt the full equilibrium CO_2 geothermometer of Giggenbach (1984) for this purpose. Both approaches provide similar results (<10°C difference) for temperatures 200-300 °C.

The histogram of TCO2 Flux is sometimes multi-modal (Wairakei, Ohaaki, Rotokawa), and this may indicate surface thermal areas supplied by vapour from distinct reservoirs. At Rotokawa and Wairakei, areas of highest TCO2 Flux are consistent with upflow locations from existing conceptual models. At Reporoa, mean TCO2 Flux (310 °C) is high, which indicates Reporoa has an upflow distinct from Waiotapu; a Waiotapu outflow would not be expected to have such high temperature.

ACKNOWLEDGMENTS

REFERENCES

Agusto, M., Tassi, F., Caselli, A. T., Vaselli, O., Rouwet, D., Capaccioni, B., Caliro, F., Chiodini, G., and Darrah, T. (2013) Gas geochemistry of the magmatic-hydrothermal fluid reservoir in the Copahue–Caviahue Volcanic Complex (Argentina). J. Volcanol. Geotherm. Res. 257, 44-56.

Allis, R. G. (1981) Changes in heat flow associated with exploitation of Wairakei geothermal field, New Zealand. New Zeal. J. Geol. Geophys. 24, 1-19.

Ármannsson, H. (2016) The fluid geochemistry of Icelandic high temperature geothermal areas. Appl. Geochem. 66, 14-64.

Armstrong, M. (1998) Basic Linear Geostatistics. Springer Science & Business Media.

Arnórsson, S. (1978) Major element chemistry of the geothermal sea-water at Reykjanes and Svartsengi, Iceland. Mineral. Mag. 42, 209.

Arnórsson, S., and Gunnlaugsson, E. (1985) New gas geothermometers for geothermal exploration—calibration and application. Geochem. Cosmochim. Acta. 49, 1307-1325.

Arnórsson, S. (1985) The use of mixing models and chemical geothermometers for estimating underground temperatures in geothermal systems. J. Volcanol. Geotherm. Res. 23, 299-335.

Arnórsson, S., Fridriksson, T., and Gunnarsson, I. (1998) Gas chemistry of the Krafla Geothermal field, Iceland. In: Arehart G.B., Hulston J.R. (Eds)., Proceedings of the 9th International Symposium Water–Rock Interaction, WRI-9, pp. 613–616.

Arnórsson, S., Bjarnason, J. Ö., Giroud, N., Gunnarsson, I., and Stefánsson, A. (2006) Sampling and analysis of geothermal fluids. Geofluids 6, 203-216.

Bibby, H. M., Bennie, S. L., Stagpoole, V. M., and Caldwell, T. G. (1994) Resistivity structure of the Waimangu, Waiotapu, Waikite and Reporoa geothermal areas, New Zealand. Geothermics 23, 445-471.

Bixley, P. F., Clotworthy, A. W., and Mannington, W. I. (2009) Evolution of the Wairakei geothermal reservoir during 50 years of production. Geothermics 38, 145-154.

Bloomberg, S., Rissmann, C., Mazot, A., Oze, C., Horton, T., Gravley, D., Kennedy, B., Werner, C., Christenson, B., and Pawson J. (2012) Soil gas flux exploration at the Rotokawa geothermal field and White Island, New Zealand, PROCEEDINGS, Thirty-Sixth Workshop on Geothermal Reservoir Engineering.

Bloomberg, S., Werner, C., Rissmann, C., Mazot, A., Horton, T., Gravley, D., Kennedy, B., and Oze, C. (2014) Soil CO_2 emissions as a proxy for heat and mass flow assessment, Taupō Volcanic Zone, New Zealand. Geochem. Geophys. Geosyst. 15, 4885–4904.

Brombach, T., J. C. Hunziker, G. Chiodini, C. Cardellini, and Marini, L. (2001) Soil diffuse degassing and thermal energy fluxes from the southern Lakki plain, Nisyros (Greece), Geophys. Res. Lett. 28, 69-72.

Bromley, C. J., and Hochstein, M. P. (2005) Heat discharge of steaming ground at Karapiti (Wairakei), New Zealand. Proc. World Geotherm. Congr. 3rd.

Browne, P. R. L., and Ellis, A. J. (1970) The Ohaki-Broadlands hydrothermal area, New Zealand; mineralogy and related geochemistry. Am. J. Sci. 269, 97-131.

Chiodini, G., F. Frondini, and Raco, B. (1996) Diffuse emission of CO2 from the Fossa crater, Vulcano Island (Italy), Bull. Volcan. 58, 41-50.

Chiodini, G., and Marini, L. (1998) Hydrothermal gas equilibria: the H 2 OH 2-CO 2-CO-CH 4 system. Geochem. Cosmochim. Acta. 62, 2673-2687.

Chiodini, G., Granieri, D., Avino, R., Caliro, S., Costa, A., and Werner, C. (2005). Carbon dioxide diffuse degassing and estimation of heat release from volcanic and hydrothermal systems. J. Geophys. Res.: Sol. Ear. 110.

Chiodini, G., Cardellini, C., Lamberti, M. C., Agusto, M., Caselli, A., Liccioli, C., Tamburello, G., Tassi, F., Vaselli, O., and Caliro, S. (2015) Carbon dioxide diffuse emission and thermal energy release from hydrothermal systems at Copahue–Caviahue Volcanic Complex (Argentina). J. Volcanol. Geotherm. Res. 304, 294-303.

Christenson, B. W., Mroczek, E. K., Kennedy, B. M., Van Soest, M. C., Stewart, M. K., and Lyon, G. (2002) Ohaaki reservoir chemistry: characteristics of an arc-type hydrothermal system in the Taupō Volcanic Zone, New Zeal. J. Volcanol. Geotherm. Res. 115, 53-82.

Dawson, G.B. (1964) The nature and assessment of heat flow from hydrothermal areas. New Zeal. J. Geol. Geophys. 7, 155-171.

DSIR (1967) Chemistry of Hole 1 Reporoa (RP-1). Chemistry Division Report, DSIR. CD.118/12 – RGB/47 AJE.

Fournier, R. O. (1977) Chemical geothermometers and mixing models for geothermal systems. Geothermics, 5, 41-50.

Freedman, A. J., Bird, D. K., Arnórsson, S., Fridriksson, T., Elders, W. A., and Fridleifsson, G. Ó. (2009) Hydrothermal minerals record CO2 partial pressures in the Reykjanes geothermal system, Iceland. Amer. J. Sci. 309, 788-833.

Fridriksson, T., B. R. Kristjánsson, H. Ármannsson, E. Margrétardóttir, S. Ólafsdóttir, and Chiodini, G. (2006) CO2 emissions and heat flow through soil, fumaroles, and steam heated mud pools at the Reykjanes geothermal area, SW Iceland, Appl. Geochem., 21, 1551-1569.

Fridriksson, T., Oladottir, A. A., Jonsson, P., and Eyjolfsdottir, E. I. (2010) The response of the Reykjanes geothermal system to 100 MWe power production: fluid chemistry and surface activity. World Geotherm. Congr. 4th.

Giggenbach, W. F. (1980) Geothermal gas equilibria. Geochem. Cosmochim. Acta 44, 2021-2032.

Giggenbach, W. F. (1981) Geothermal mineral equilibria. Geochem. Cosmochim. Acta 45, 393-410.

Giggenbach, W. F. (1984) Mass transfer in hydrothermal alteration systems—a conceptual approach. Geochem. Cosmochim. Acta 48, 2693-2711.

Giggenbach, W. (1987) Redox processes governing the chemistry of fumarolic gas discharges from White Island, New Zealand. Appl. Geochem. 2, 143–161.

Giggenbach, W. F. (1988) Geothermal solute equilibria. derivation of Na-K-Mg-Ca geoindicators. Geochem. Cosmochim. Acta 52, 2749-2765.

Giggenbach, W.F. (1989) The chemical and isotopic position of the Ohaaki field within the Taupo Volcanic Zone. p. 81–88. In: Browne, P.R.L., Nicholson, K.(Eds.), Proc. New Zeal. Geotherm. Workshop, 11th.

Giggenbach, W. F. (1995) Variations in the chemical and isotopic composition of fluids discharged from the Taupo Volcanic Zone, New Zealand, J. Volcanol. Geotherm. Res. 68, 89-116.

Giggenbach, W., H. Shinohara, M. Kusakabe, and Ohba, T. (2003) Formation of acid volcanic brines through interaction of magmatic gases, seawater, and rock within the White Island volcanic-hydrothermal system, New Zeal. Spec. Publ. Soc. Econ. Geol. 10, 19–40.

Glover, R. B., Mroczek, E. K., and Finlayson, J. B. (2001) Fumarolic gas chemistry at Wairakei, New Zealand, 1936–1998. Geothermics 30, 511-525.

Glover, R. B. and Mroczek, E. K. (2009) Chemical changes in natural features and well discharges in response to production at Wairakei, New Zealand, Geothermics 38, 117-133.

Gudmundsdottir, A.L. (1988) Natural heat flow through surface in geothermal areas in the Nesjavellir area. University of Iceland 4th year honors thesis.

Harvey, C. C., and Browne, P. R. (1991). Mixed-layer clay geothermometry in the Wairakei geothermal field, New Zealand. Clays and Clay Min. 39(6), 614-621.

Harvey, M. C., Rowland, J. V., Chiodini, G., Rissmann, C. F., Bloomberg, S., Hernández, P. A., Mazot, A., Viveiros, F., and Werner, C. (2015a) Heat flux from magmatic hydrothermal systems related to availability of fluid recharge. J. Volcanol. Geotherm. Res. 302, 225-236.

Harvey, M. C., Zygadlo, M., and Dwivedi, A. (2015b) Use of isotopic analysis to distinguish between biological and geothermal soil CO2 flux at Tauhara and Te Mihi geothermal areas. Proc. New Zeal. Geotherm. Workshop, 37th.

Hatherton, T., Macdonald, W. J. P., and Thompson, G. E. K. (1966) Geophysical methods in geothermal prospecting in New Zealand. Bull. Volcanologique 29, 485-497.

Harvey et al.

Healy, J., and Hochstein, M. P. (1973) Horizontal flow in hydrothermal systems. J. Hydrol. New Zeal. 12, 71-82.

Hedenquist, J. W. (1990) The thermal and geochemical structure of the Broadlands-Ohaaki geothermal system, New Zealand. Geothermics 19, 151-185.

Hedenquist, J. W., S. F. Simmons, W. F. Giggenbach, and Eldridge, C. S. (1993) White Island, New Zealand, volcanic-hydrothermal system represents the geochemical environment of high-sulfidation Cu and Au ore deposition, Geology 21, 731-734.

Henley, R. W., Truesdell, A. H., Barton, P. B., and Whitney, J. A. (1984) Fluid-mineral equilibria in hydrothermal systems (Vol. 1). El Paso, TX: Society of Economic Geologists.

Hernández, P. A., N. M. Pérez, T. Fridriksson, J. Egbert, E. Ilyinskaya, A. Thárhallsson, G. Ívarsson, G. Gíslason, I. Gunnarsson, and Jónsson, B. (2012), Diffuse volcanic degassing and thermal energy release from Hengill volcanic system, Iceland, Bull. Volcan. 74, 2435-2448.

Hochstein, M. P. and Bromley C. J. (2005), Measurement of heat flux from steaming ground, Geotherm. 34, 131-158.

Houghton, B., and Nairn, I. (1991) The 1976–1982 Strombolian and phreatomagmatic eruptions of White Island, New Zealand: eruptive and depositional mechanisms at a 'wet' volcano. Bull. Volcanol. 54, 25–49.

McNamara, D. D., Sewell, S., Buscarlet, E., and Wallis, I. C. (2016) A review of the Rotokawa Geothermal Field, New Zealand. Geothermics 59, 281-293.

Mroczek, E. K., Lee, S. G., Smith, R., Carey, B. (2008) Ohaaki West Bank production fluid compositions. Proc. New Zeal. Geotherm. Workshop, 30th.

Mroczek, E. K., Milicich, S. D., Bixley, P. F., Sepulveda, F., Bertrand, E. A., Soengkono, S., and Rae, A. J. (2016) Ohaaki geothermal system: Refinement of a conceptual reservoir model. Geothermics 59, 311-324.

Pullar, W. A., Birrell, K. S., and Heine, J. C. (1973) Named tephras and tephra formations occurring in the central North Island, with notes on derived soils and buried paleosols. New Zeal. J. Geol. Geophys. 16, 497-518.

Risk, G. F., Caldwell, T. G., and Bibby, H. M. (1994) Deep resistivity surveys in the Waiotapu-Waikite-Reporoa region, New Zealand. Geothermics 23, 423-443.

Rissmann, C.F.W., (2010) Using surface methods to understand the Ohaaki Hydrothermal Field, Taupo Volcanic Zone, New Zealand. In: PhD Thesis at the Department of Geological Sciences. University of Canterbury.

Rissmann, C., B. Christenson, C. Werner, M. Leybourne, J. Cole, and Gravley, D. (2012) Surface heat flow and CO2 emissions within the Ohaaki hydrothermal field, Taupō Volcanic Zone, New Zealand, Appl. Geochem. 27, 223-239.

Robert, C., and Casella, G. (2013) Monte Carlo Statistical Methods. Springer Science and Business Media.

Rowland, J. V., and Sibson, R. H. (2004) Structural controls on hydrothermal flow in a segmented rift system, Taupō Volcanic Zone, New Zealand. Geofluids 4, 259-283.

Rosenberg, M. D., Bignall, G., and Rae, A. J. (2009) The geological framework of the Wairakei–Tauhara geothermal system, New Zealand. Geothermics 38, 72-84.

Rosenberg, M., Wallin, E., Bannister, S., Bourguignon S.. Sherburn, S., Jolly, G., Mroczek, E., Milicich, S., Graham, D., Bromley, C., Reeves, R., Bixley, P., Clothworthy, A., Carey, B., Climo, M., and Links, F. (2010) Tauhara Stage II Geothermal Project: Geo-Science report. In: GNS Science Consultancy Report 2010/138, February, 2010, http://www.contactenergy.co.nz/aboutus/pdf/environmental/P3GeoscienceReport.pdf

Sepúlveda, F., Rosenberg, M. D., Rowland, J. V., and Simmons, S. F. (2012) Kriging predictions of drill-hole stratigraphy and temperature data from the Wairakei geothermal field, New Zealand: Implications for conceptual modeling. Geothermics 42, 13-31.

Simpson, M. P., and Bignall, G. (2016) Undeveloped high-enthalpy geothermal fields of the Taupō Volcanic Zone, New Zealand. Geothermics 59, 325-346.

Stefánsson, A., and Arnórsson, S. (2002) Gas pressures and redox reactions in geothermal fluids in Iceland. Chem. Geol. 190, 251-271.

Steiner, A. (1977) The Wairakei geothermal area, North Island, New Zealand: its subsurface geology and hydrothermal rock alteration (No. 90). New Zealand Dept. of Scientific and Industrial Research.

Takenouchi, S., and Kennedy, G. C. (1964) The binary system H2O-CO2 at high temperatures and pressures. Amer. J. Sci. 262, 1055-1074.

Werner, C.A., Hochstein, M.P., and Bromley, C.J. (2004) CO2-flux of steaming ground at Karapiti, Wairakei. Proc. New Zeal. Geotherm. Workshop. 26th.

Werner, C., and Cardellini, C. (2006) Comparison of carbon dioxide emissions with fluid upflow, chemistry, and geologic structures at the Rotorua geothermal system, New Zealand. Geothermics 35, 221-238.

Werner, C., Chiodini, G., Granieri, D., Caliro, S., Avino, R., and Russo, M. (2006) Eddy covariance measurements of hydrothermal heat flux at Solfatara volcano, Italy. Earth Planet. Sci. Lett. 244, 72-82.

Wilson, C. J., and Rowland, J. V. (2016) The volcanic, magmatic and tectonic setting of the Taupō Volcanic Zone, New Zealand, reviewed from a geothermal perspective. Geothermics 59, 168-187.

Winick, J., Powell, T., and Mroczek, E. (2009) The natural state chemistry of the Rotokawa reservoir. *Proc. New Zeal. Geotherm. Workshop*, *31*st.